ISSN: 0067-2904
GIF: 0.851

The Relationship Between Solar Indices and Electron Density of D- Region over Baghdad City During the Ascending and the Descending Phases of Solar Cycle 23

Fahmi A. Mohammed*
Department of Space Environment, Atmosphere and Space Science Center, Directorate of Space and Communications, Ministry of Science and Technology, Baghdad, Iraq

Abstract

This research dedicated to make an investigation for the variation of electron density concentration of D- region(NmD), at a characteristic height of 81 km throughout solar cycle 23, with solar activity(represented by sunspot number indices: international sunspot number(Ri), Northern hemisphere sunspot number(Rn) and Southern hemisphere sunspot number(Rs), as well as, the correlation between these indices for Baghdad city(lat.: 33.3^o N, long.: 44.4^o E) at local noon time during the ascending and the descending phases of solar cycle 23. A very strong directly relationship were found between Ri, Rn and Rs with NmD, as well as, the correlation coefficient between these parameters have been calculated and it has been found it is equal, i.e., the three solar indices can be depend on them for predicting NmD.

Keywords: international sunspot number(Ri), Northern hemisphere sunspot number(Rn), Southern hemisphere sunspot number(Rs), Electron density of D-region, Ascending phase of solar cycle 23, Descending phase of solar cycle 23.

العلاقة بين المعاملات الشمسية والكثافة الالكترونية لمنطقة D فوق مدينة بغداد خلال الطورين المرتفع والمنخفض من الدورة الشمسية 23

فهمي عبد الرحمن محمد*
قسم بيئة الفضاء، مركز علوم الجو والفضاء، دائرة الفضاء والاتصالات، وزارة العلوم والتكنولوجيا، بغداد، العراق

الخلاصة

هذا البحث مخصص لاجراء دراسة حول تغير تركيز الكثافة الالكترونية لمنطقة D الايونوسفيرية (NmD) ، عند ارتفاع ثابت (81 km) على طول الدورة الشمسية 23، مع النشاط الشمسي(المتمثل بمعاملات عدد البقع الشمسية: عدد البقع الشمسية العالمي، Ri ، عدد البقع الشمسية في النصف الشمالي من الشمس،Rn ، وعدد البقع الشمسية في النصف الجنوبي من الشمس، Rs)، بالاضافة الى، العلاقة بينهم لمدينة بغداد(خط عرض: 33.3 درجة شمالا، خط طول: 44.4 درجة شرقا) عند الظهر المحلي خلال الطورين المرتفع والمنخفض من الدورة الشمسية 23 . وجد بأن هناك علاقة طردية قوية جدا بين Ri, Rn and Rs مع NmD بالاضافة الى وجود معامل ارتباط متساوي بينهم، بمعنى ان المعاملات الشمسية الثلاثة يمكن الاعتماد عليها في تنبؤ NmD .

1- Introduction:

The International Reference Ionosphere (IRI) project was initiated by the Committee on Space Research (COSPAR) and by the International Union of Radio Science (URSI) in the late sixties of last century with the goal of establishing an international standard for the specification of ionospheric parameters based on all worldwide available data from ground- based and satellite observations.

*Email:fahmibeg@yahoo.com

IRI describes monthly averages of ionospheric densities in the altitude range of 50- 1500 km in the non- auroral ionosphere. One of the most important data sources for the IRI electron density is the worldwide network of ionosonde stations which has monitored the ionosphere with varying station density since the nineteen- thirties. Besides the ionosonde network, other data sources for the IRI model development include the incoherent scatter (IS) radars, several compilations of rocket measurements, and satellite data from in situ and topside sounder instruments. The IS radars measures all the IRI parameters over the full altitude range, but only a few radars are in operation worldwide. Their data are essential for the description of variations with time, season, and solar activity, whereas the satellite data are a primary source for the description of the global morphology of ionospheric parameters. In the lower ionosphere, the large neutral densities make radar and satellite measurements very difficult or impossible and rocket flight are the prime data source for IRI [1]. The IRI generally describes the E & D- region electron density well, but it does not yet include the ionization enhancement at auroral latitudes caused by precipitating particles. For the non- auroral D- region, IRI offers three different options: (1) the standard model based on a small selection of representative rocket profiles [2]. (2) The FIRI model based on a compilation of rocket data with simultaneous radio propagation and in situ measurements[3] and (3) the Danilov et al. (1995) model [4] based on a compilation of Russian rocket data not included in the FIRI set [5]. Various authors have investigated the dependence of electron density on solar activity, in the lower part of the D- region (a characteristic height of 60 km). Some authors obtained an increase in electron density with solar activity, while others obtained a decrease. The D- region electron concentration dependence on solar activity was studied on the basis of 80 rocket measurements in Thumba by a probe method. The rockets were flown under solar zenith angles of $\chi = 71^{o} \pm 2$ in 1979- 1990 and 1984- 1987. This set of data made it possible to conclude that the sign of the solar activity affect changes with altitude: electron density decreases with F (10.7 cm) increase in the lowest D- region and increases in the upper D- region [6]. On the basis of 14 rocket probe measurement of electron density at Thumba (8^{o} N) in 1979- 1980 [F(10.7 cm) which varied from 139 to 243], Pakhomov obtained a positive correlation between electron density and F(10.7 cm) at 75 km, with a correlation coefficient of 0.77 [7].

The F(10.7 cm) solar radio flux is the flux of radio waves emitted by the sun at a wavelength of 10.7 cm(2800 MHz frequency) in units of 10^{4} Jansky (a Jansky is defined as 10^{-26} W m^{-2} Hz^{-1} bandwidth), and is used as a proxy for extreme ultraviolet (EUV) radiation, which heats the upper atmosphere and cannot be measured from the ground.

Danilov *et al.*, obtained a well- pronounced increase in electron density with solar activity, at 90 km[8]. Danilov considered the problem of solar activity impact on the D- region from a general point of view. He showed that from physical considerations one can expect a weak increase in electron density with solar activity in the upper part of the D- region, which is, difficult to detect [9]. Bremer and Singer studied solar cycle variations of electron densities in the ionospheric D- regions, and the results showed a general enhancement of electron density with increasing solar activity in the whole height region[10]. Mechtly *et al.*, compared the probe measurements (calibrated to onboard Faraday data) of five rocket flights in April- December 1965 (low solar activity) with five flights in July- December 1969 (high solar activity). The measurements were conducted at Wallops Island, 38^{o} N under solar zenith angles of about 60^{o}, they concluded that at all the altitudes considered (70- 90 km), electron density increased with solar activity [11]. McNamara found unusual electron density dependence on solar activity: an increase in electron density by 1.6 times (under increase in Ri from 0 to 100) at 60 and 80 km and almost complete absence of the effect at 70 and 90 km [12].

Smirnova *et al.*, studied the electron density variations at various heights in Summer at the 50^{o} N latitude. They predicted a decrease in electron density with solar activity in the lower part of the D- region and an increase in the upper part [13, 14].

2- Theory:

2- 1 Solar activities:

Any change in the Sun's appearance or behaviour. The Sun's activity is described as being very low, low, moderate, high or very high.

2-1-1 The solar wind:

The Sun is constantly ejecting material from its surface in all directions into space, making up the so- called solar wind. Under relatively quiet solar conditions the solar wind blows around 200 miles per second- 675,000 miles per hour- taking away about two million tons of solar material each second

from the Sun. The density of the material in the solar wind is very small by the time it has been spread out into interplanetary space.

2-1-2 Sunspots:

Radio propagation phenomena vary with the number and size of sunspots, and also with the position of sunspots on the surface of the Sun. There are daily and seasonal variations in the Earth's ionized layers resulting from changes in the amount of ultraviolet light received from the Sun. The 11-year sunspot cycle affects propagation conditions because there is a direct correlation between sunspot activity and ionization.

Individual sunspots may vary in size and appearance, or even disappear totally, within a single day. In general, larger active areas persist through several rotations of the Sun. Some active areas have been identified over periods up to about a year. Because of these continual changes in solar activity, there are continual changes in the state of the Earth's ionosphere and resulting changes in propagation conditions.

2-1-3 Solar flares:

Solar flares are cataclysmic eruptions that suddenly release huge amounts of energy, including sustained, high- energy bursts of radiation from very low frequency (VLF) to X- ray frequencies and vast amounts of solar material. Most solar flares occur around the peak of the 11- year solar cycle. If the geometry between the Sun and Earth is right, intense X- ray radiation takes eight minutes, traveling the 93 million miles to Earth at the speed of light. The sudden increase in X- ray energy can immediately increase radio frequency (RF) absorption in the Earth's lowest ionospheric layers, causing a phenomenon known as a Sudden Ionospheric Disturbance (SID). This phenomenon affects all high frequency (HF) communications on the sunlit side of the Earth.

Between 45 minutes and 2 hours after an SID begins, particles from the flare begin to arrive. These high- energy particles are mainly protons and they can penetrate the ionosphere at the Earth's magnetic poles, where intense ionization can occur, with attendant absorption of HF signals propagating through the polar regions. This is called a Polar Cap Absorption(PCA) event and it may last for several days [15].

2-2 Solar Cycle 23:

This cycle lasted 11.6 years, beginning in 1996 and ending in 2008. The ascending phase of solar cycle ranges from 1996 to 2000, while the descending phase from 2001 to 2008. The maximum smoothed sunspot number (monthly number of sunspots averaged over a twelve- month period) observed during the solar cycle was 120.8 (March 2000), and the minimum was 1.7 . The maximum yearly smoothed number of sunspot was 119.6 (2000), and the minimum was 2.9 (2008). The maximum yearly smoothed number of sunspot in the Northern hemisphere of the Sun was 61.25 (2000), and the minimum was 0.72 (2008). The maximum yearly smoothed number of sunspot in the Southern hemisphere of the Sun was 57.4 (2002), and the minimum was 2.1 (2008). A total of 805 days had no sunspots during this cycle.

2-3 Structure of the ionosphere:

The ionosphere is composed of a number of ionized regions above the Earth’s surface which play a most important part in the propagation of radio waves. These regions are influence on radio waves mainly because of the presence of free electrons, which are arranged in approximately horizontally stratified layers. For reasons related to the historical development of ionospheric research, the ionosphere is divided into three regions or layers designated D, E and F, respectively, in order of increasing altitude. Subdivisions of these regions may exist under certain conditions, for example F1 and F2 layers. From the viewpoint of HF propagation, the E- and F- regions act mainly as radio wave reflectors, and permit long range propagation between terrestrial terminals. The D- region acts principally as an absorber, causing signal attenuation in the HF range, although very low frequency (VLF) and extremely low frequency (ELF) waves are reflected at D- region altitudes.

The ionospheric structure varies widely over the Earth’s surface, since the strength of the sun’s radiation varies considerably with geographic latitude.

2-3-1 Ionization:

The principal source of ionization in the ionosphere is electromagnetic radiation emitted from the sun extending over the ultra- violet and X- ray portions of the spectrum. Other sources of ionization are important, however, such as energetic charged particles of solar origin and galactic cosmic rays. The ionization rate at various altitudes depends upon the intensity of the solar radiation (as a function

of wavelength) and the ionization efficiency of the neutral atmospheric gases. Since the sun's radiation is progressively absorbed in passing through the atmosphere, its residual ionizing ability depends upon the length of the atmospheric path, and consequently upon the solar zenith angle (φ). The maximum ionization rate occurs when the sun is overhead (φ = 0), but geographic, diurnal and seasonal variations in the ionization density are found. The production of free ionization by solar radiation (and charged particles) is counter- balanced by ionization loss processes, principally the collisional recombination of electrons and positive ions, and the attachment of electrons to neutral gas atoms and molecules.

2-3-2 D- region:

The D- region spans the approximate altitude range 50– 90 km with electron concentration increasing rapidly with altitude. The D- region electron density exhibits large diurnal variations. It has a maximum value shortly after local solar noon and a very small value at night. This diurnal variation is greatest in the altitude interval 70– 90 km, with typical noon values of 10^8– 10^9 electrons/m^3. There is a pronounced seasonal variation in D- region electron densities with a maximum in summer.

The relatively high density of the neutral atmosphere in the D- region causes the electron collision frequency to be correspondingly high (~2×10^6 sec^{-1} at 75 km). It is therefore in this region that the main absorption of energy from a propagating radio wave takes place.

2-3-3 E- region:

The altitude range from 90– 130 km constitutes the E- region and encompasses the so- called 'normal' and 'sporadic' E- layers. The former is a regular layer which displays a strong solar zenith angle dependence with maximum density near noon and a seasonal maximum in summer. The altitude of maximum density is about 110 km, with a value of the order of 10^{11} electrons/m^3. At night only a small residual level of ionization remains in the E- region. The solar cycle dependence exhibits a maximum layer density at solar sunspot maximum. The normal E layer is important for daytime HF propagation at distances less than 2000 km.

Sporadic E manifests itself in enhanced ionization at E- region heights causing much greater critical frequencies when it is present. Its occurrence is strongly latitude dependent; in central European latitudes it is more frequent in summer than in winter and more frequent by day than by night. In high latitudes it is essentially a night- time phenomenon, in low latitudes a daytime one. Sporadic E occasionally prevents frequencies that normally penetrate the E- layer from reaching higher layers and sometimes causes long-distance transmission at very high frequencies.

2-3-4 F- region:

The F- region extends upwards from about 130 km and is divided into the F1 and F2 layers, although this distinction is only apparent during daytime. The F1 layer is the region between 130– 210 km altitude, in which the maximum electron density is about $2\times10^{11}/m^3$. It exists only during daylight. This layer is occasionally the reflecting region for HF transmission, but more usually obliquely-incident waves that penetrate the E- region also penetrate the F1 layer and are reflected by the F2 layer. The F1 layer introduces additional absorption of such waves.

The F2 layer is the highest ionospheric layer, and usually exhibits the greatest electron density, which may range typically from $10^{12}/m^3$ in daytime to about $5\times10^{10}/m^3$ at night. The F2 layer is not well represented by a simple model since it is strongly influenced by winds, diffusion and other dynamic effects.

Ranging in height between about 250 to 400 km, the F2 layer is the principal reflecting region for long distance HF communication. Height and ionization density vary diurnally, seasonally and over the sunspot cycle. Ionization does not follow the solar zenith angle in any fashion since with such low molecular collision rates the medium can store received solar energy for many hours. At night the F1 layer merges with the F2 layer at a height of about 300 km. The absence of the F1 layer and reduction in absorption of the E- region causes night- time field intensities and noise to be generally higher than during daylight.

Some special features of the F- region occur at low and high latitudes; these can have important effects upon radio wave propagation. Near the equator significant latitudinal gradients exist in the F-region ionization whilst at high latitudes there is a region of strongly depressed electron density [16].

3-Collection of data:

The records of Northern and Southern hemispheric sunspot number data, started on 1/1/1992 up to now. Since, the period of solar cycle 23 ranges from 1996 to 2008 (12 years), hence, solar cycle 23 has been chosen in this work.

Yearly mean values of solar indices, Ri(smoothed), Rn(smoothed) and Rs(smoothed), were obtained from Solar Influences Data Center(SIDC) [17]; while yearly mean values of NmD were obtained from IRI- 2012 model (http://omniweb.gsfc.nasa.gov/vitmo/iri2012_vitmo.html), by inputting each value of solar indices mentioned for each year from 1996 to 2008, as shown in tables (1- 6). .

4- Results and discussion:

Figures-4 to 6 show the directly increasing of yearly mean values of solar indices (Ri, Rn and Rs), respectively as a function of yearly mean values of electron density concentration of D- region for Baghdad at local noon time during the ascending phase of solar cycle 23. Figures -7 to 9 demonstrate the directly increasing of yearly mean values of solar indices(Ri, Rn and Rs), respectively as a function of yearly mean values of electron density concentration of D- region for Baghdad at local noon time during the descending phase of solar cycle 23.

Table 1- Yearly mean values of Ri (smoothed) with NmD during the ascending phase of solar cycle 23

Years	Ri(smoothed)	NmD($*10^8$ m^{-3})
1996	8.6	4.17
1997	21.5	4.87
1998	64.3	7.18
1999	93.3	8.74
2000	119.6	10.1

Table 2- Yearly mean values of Rn (smoothed) with NmD during the ascending phase of solar cycle 23

Years	Rn(smoothed)	NmD($*10^8$ m^{-3})
1996	4.49	4
1997	11.68	4.34
1998	30.58	5.36
1999	52.37	6.53
2000	61.25	7.01

Table 3- Yearly mean values of Rs (smoothed) with NmD during the ascending phase of solar cycle 23

Years	Rs(smoothed)	NmD($*10^8$ m^{-3})
1996	4.55	4
1997	10.93	4.3
1998	31.75	5.42
1999	42.92	6.02
2000	55.54	6.71
2001	52.58	6.55
2002	57.4	6.81

Table 4- Yearly mean values of Ri (smoothed) with NmD during the descending phase of solar cycle 23

Years	Ri(smoothed)	NmD($*10^8$ m^{-3})
2001	111	9.7
2002	104	9.32
2003	63.7	7.15
2004	40.4	5.89
2005	29.8	5.32
2006	15.2	4.53
2007	7.5	4.11
2008	2.9	4

Table 5- Yearly mean values of Rn (smoothed) with NmD during the descending phase of solar cycle 23

Years	Rn(smoothed)	NmD($*10^8$ m^{-3})
2001	57.95	6.84
2002	44.25	6.1
2003	28.31	5.24
2004	14.84	4.51
2005	10.4	4.27
2006	3.03	4
2007	0.98	4
2008	0.72	4

Table 6-Yearly mean values of Rs (smoothed) with NmD during the descending phase of solar cycle 23

Years	Rs(smoothed)	NmD($*10^8$ m^{-3})
2003	37.23	5.72
2004	27.02	5.17
2005	18.5	4.71
2006	12.98	4.41
2007	6.97	4.08
2008	2.1	4

It is seen from Table-1 that the NmD values increased with increasing of Ri from the beginning to the peak of solar cycle with ($5.93*10^8$ m^{-3}); and decreased from the peak to the end of solar cycle with ($5.7*10^8$ m^{-3}) as shown from Table-4, and the magnitude of increasing of NmD is greater than the magnitude of decreasing with ($0.23*10^8$ m^{-3}). And it is seen from Table-2 that the NmD values

increased with increasing of Rn from the beginning to the peak of solar cycle with ($3.01*10^8$ m^{-3}); and decreased from the peak to the end of solar cycle with ($2.84*10^8$ m^{-3}) as shown from Table-5, and the magnitude of increasing of NmD is greater than the magnitude of decreasing with ($0.17*10^8$ m^{-3}).

The variation of NmD corresponding to Ri and Rn is uniform with one peak along the solar cycle 23(the ascending and the descending phases of solar cycle 23), as shown in Figures-1 and 2.

A two peaks of solar cycle were found (the first peak in 2000 at which maximum value of Rs is 55.54 and corresponds to a highest value of NmD ($6.71*10^8$ m^{-3}), and the second peak in 2002 at which maximum value of Rs is 57.4 and corresponds to a highest value of NmD ($6.81*10^8$ m^{-3}), as shown in Figure-3.

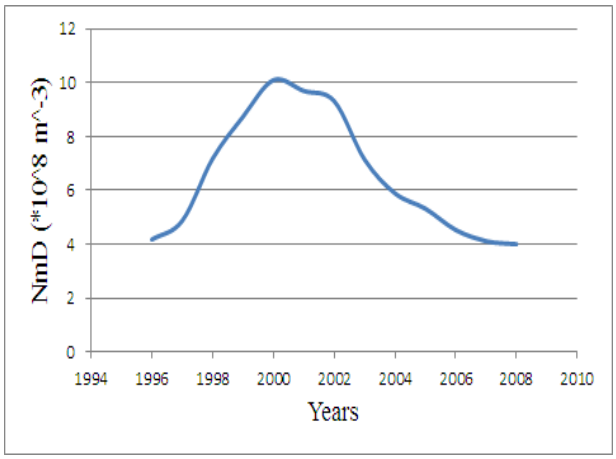

Figure 1-Variation of NmD values corresponding to Ri values for Baghdad during the ascending and descending phases of solar cycle 23

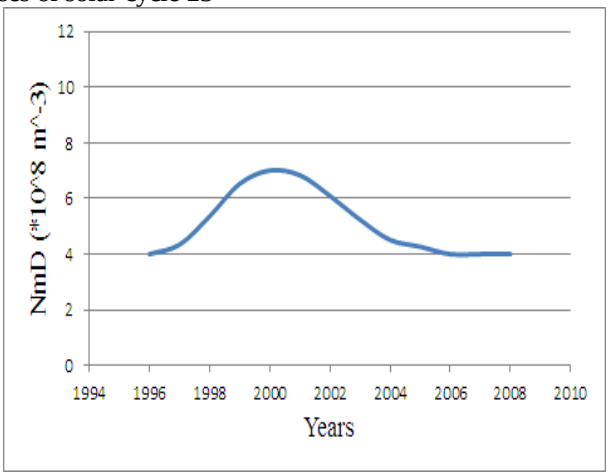

Figure 2- Variation of NmD values corresponding to Rn values for Baghdad during the ascending and descending phases of solar cycle 23.

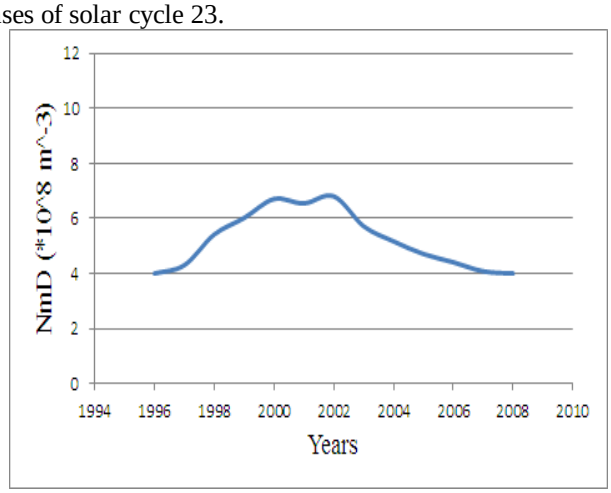

Figure 3- Variation of NmD values corresponding to Rs values for Baghdad during the ascending and descending phases of solar cycle 23.

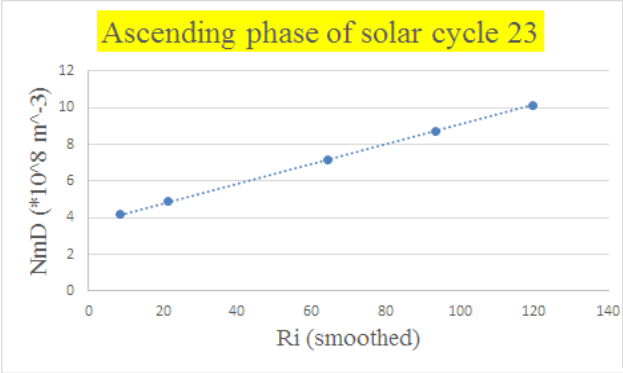

Figure 4- The electron density (NmD) as a function of international sunspot number (Ri) for the city of Baghdad at local noon time during 1996- 2000

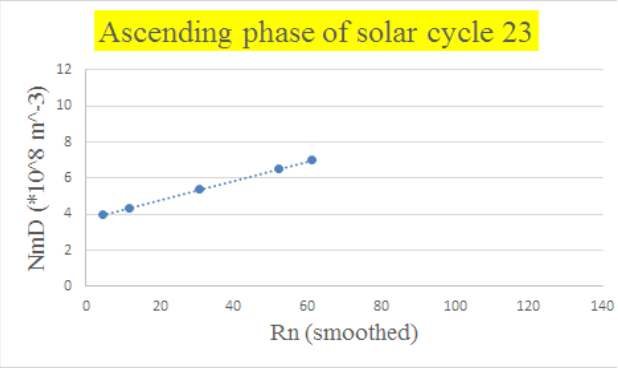

Figure5- The electron density (NmD) as a function of northern hemisphere sunspot number (Rn) for the city of Baghdad at local noon time during 1996- 2000

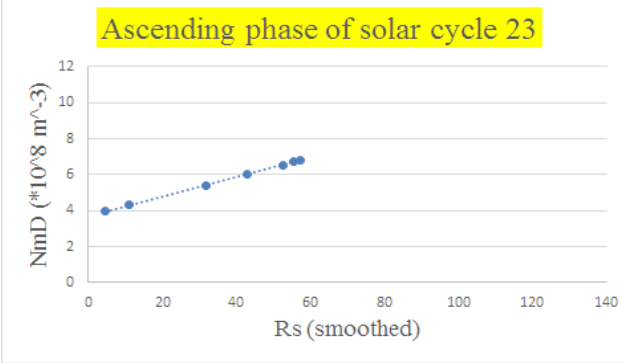

Figure 6- The electron density (NmD) as a function of southern hemisphere sunspot number (Rs) for the city of Baghdad at local noon time during 1996- 2002

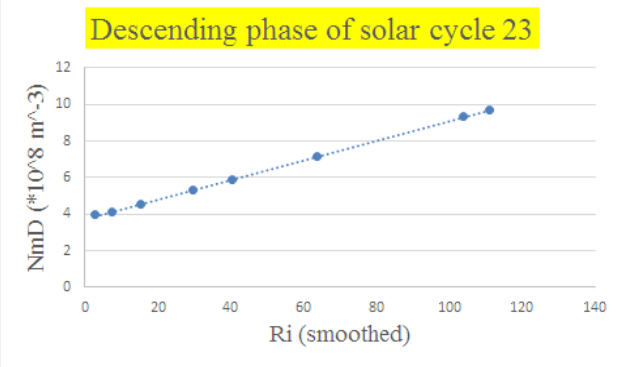

Figure 7-The electron density (NmD) as a function of international sunspot number (Ri) for the city of Baghdad at local noon time during 2001-2008

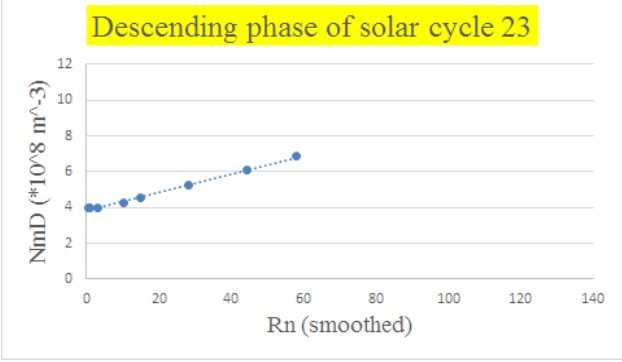

Figure 8- The electron density (NmD) as a function of northern hemisphere sunspot number (Rn) for the city of Baghdad at local noon time during 2001- 2008

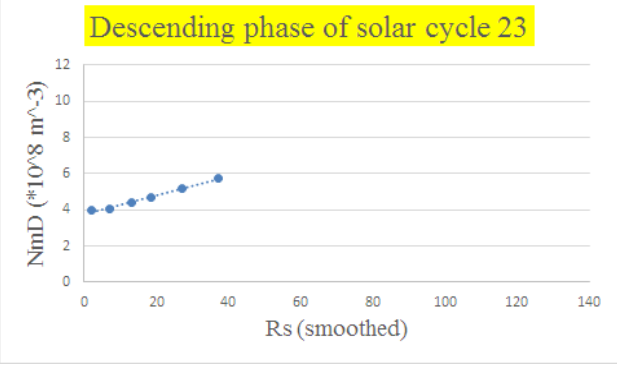

Figure 9- The electron density (NmD) as a function of southern hemisphere sunspot number (Rs) for the city of Baghdad at local noon time during 2003- 2008

Table 7- Correlation coefficient values (R) between Ri- NmD, Rn- NmD and Rs- NmD for Baghdad during the ascending and the descending phases of solar cycle 23

Solar cycle phases	Ri- NmD	Rn- NmD	Rs- NmD
Ascending phase of solar cycle 23 (1996- 2000)	0.99	0.99	0.99
Descending phase of solar cycle 23 (2001- 2008)	0.99	0.99	0.99

Since the data are theoretically calculated from IRI- 2012 model, all the points, during the ascending and the descending phases, lie on the same straight line as demonstrated in Figures-4 to 9.

Conclusions:

1. There is a strong relationship between sunspot number indices and NmD during the ascending and the descending phases of solar cycle 23.
2. Correlation coefficient values for Ri, Rn and Rs with NmD during the ascending and the descending phases of solar cycle 23 are the same.
3. The electron density for D- region increases with Rn by the same value as with Rs for the ascending phase of solar cycle 23.
4. The values of the increasing and the decreasing of electron density with Rn during the ascending and the descending phases of the solar cycle 23 respectively are the same**.**

References:

1. Friedrich, M. and Torkar, K**. 2001.** FIRI: a semi empirical model of the lower ionosphere. *Journal of Geophys. Res.*, 106 (A10), pp: 21409- 21418.
2. Mechtley, E. and Bilitza, D**. 1974.** Models of D- region electron concentration, *Rep. IPW- WB1. Inst. fu¨r phys*. Weltraumforsch Freiburg, Germany.
3. Friedrich, M., Pilgram, R. and Torkar, K**. 2001.** A novel concept for empirical D- region modeling, *Adv. Space Res.*, 27(1), pp:5- 12.
4. Danilov, A. and Smirnova, N**. 1995.** Improving the 75 km to 300 km ion composition model of the IRI, *Adv. Space Res.*, 15(2), pp:171- 178.
5. Bilitza, D. and Reinisch, B.W**. 2008.** International Reference Ionosphere 2007: Improvements and new parameters, *Adv. Space Res.*, 42, pp:599- 609.
6. Danilov, A.D**. 1998.** Solar activity effects in the ionospheric D- region, *Ann. Geophysicae*, 16, pp:1527- 1533.
7. Pakhomov, S.V. and Gorbunov, A.N**. 1983.** The n(h)- profiles in the D- region of the equatorial zone (in Russian), *Geomagn. Aeron.*, pp: 23, 134.
8. Danilov, A.D., Rodevich, A.Y. and Smirnova, N.V**. 1995.** Problems with incorporating a new D-region model into the IRI, *Adv. Space Res.*, 15, p:165.
9. Danilov, A.D**. 1989.** General overview of the solar activity effects in the lower ionosphere, *Aeron. Rep.*, 29, pp:183.
10. Bremer, J. and Singer, W**. 1977.** Diurnal, seasonal and solar- cycle variations of electron densities in the ionospheric D- and E- regions, *Journal of Atmos. Sol- Terr. Phys.*, 39, pp: 25- 34.
11. Mechtly, E.A., Bowhill, S.A. and Smith, L.G**. 1972.** Changes of lower ionosphere electronconcentration with solar activity, *Journal of Atmos. Sol- Terr. Phys.*, 34, pp:1899.
12. McNamara, L.F**. 1979.** Statistical model of the D- region, *Radio Sci.*,1, p: 1165.
13. Smirnova, N.V., Ogloblina, O.F. and Vlaskov, V.A**. 1984.** Models of the electron concentration in the ionospheric D- region, Preprint PG1- 84- 08- 36, Apatity.
14. Smirnova, N.V., Ogloblina, O.F. and Vlaskov, V.A**. 1988.** Modeling of the lower ionosphere, *PAGEOF*, 127, p: 353.
15. Hathaway, D.H**. 2015.** The solar cycle. NASA Ames Research Center, CA 94035, U.S.A.
16. Maslin, N.M**. 2005.** HF communications: A system approach. Pitman Publishing, London.
17. http://www.sidc.oma.be/silso/datafiles. **2016**.